Ginsenoside Rb1 Induces a Pro-Neurogenic Microglial Phenotype via PPARγ Activation in Male Mice Exposed to Chronic Mild Stress

Zili You (youzili@uestc.edu.cn)
University of Electronic Science and Technology of China https://orcid.org/0000-0002-7776-6229
Lijuan Zhang
UESTC: University of Electronic Science and Technology of China
Minmin Tang
UESTC: University of Electronic Science and Technology of China
Xiaofang Xie
Chengdu College of Traditional Chinese Medicine: Chengdu University of Traditional Chinese Medicine
Qiuying Zhao
UESTC: University of Electronic Science and Technology of China
Nan Hu
UESTC: University of Electronic Science and Technology of China
Hui He
UESTC: University of Electronic Science and Technology of China
Gangcai Liu
UESTC: University of Electronic Science and Technology of China
Shiqi Huang
UESTC: University of Electronic Science and Technology of China
Cheng Peng
Chengdu University of Traditional Chinese Medicine Wenjiang Campus: Chengdu University of Traditional Chinese Medicine
Ying Xiao
UESTC: University of Electronic Science and Technology of China

Research Article

Keywords: Ginsenoside Rb1, Major depressive disorder, Microglia, Pro-neurogenic phenotype, Neurogenesis, Antidepressant

Posted Date: March 4th, 2021

DOI: https://doi.org/10.21203/rs.3.rs-269050/v1

Version of Record: A version of this preprint was published at Journal of Neuroinflammation on August 9th, 2021. See the published version at https://doi.org/10.1186/s12974-021-02185-0.

Abstract

Background

Anti-inflammatory approaches are emerging as a new strategy for treatment of depressive disorders. Ginsenoside Rb1 (GRb1), a major component of Panax ginseng, can inhibit inflammatory cascade and alleviate depressive behaviors. Microglia can promote or inhibit adult hippocampal neurogenesis according to their functional phenotypes. Here, we examined whether GRb1 may exert antidepressant effects by promoting a pro-neurogenic phenotype of microglia and thereby increasing neurogenesis.

Methods

The antidepressant effects of GRb1 or the licensed antidepressant imipramine (IMI) were assessed in chronic mild stress (CMS)-exposed male mice. The depressive-like behaviors of mice were evaluated by sucrose preference test, forced swimming test (FST), and tail suspension test (TST). The microglial phenotypes were identified by molecular markers and morphological properties, analyzed by RT-qPCR, western blotting and immunofluorescence staining. Effect of GRb1-treated microglia on adult hippocampal neurogenesis *in vivo* and *in vitro* were detected using immunofluorescence staining.

Results

Behavioral assessment indicated that GRb1 or IMI treatment alleviated depressive-like behaviors in CMS-exposed mice. Immunofluorescence examination

demonstrated that GRb1 induced a pro-neurogenic phenotype of microglia via activating PPARγ *in vivo* and *in vitro*, which were reversed by PPARγ inhibitor GW9662. In addition, GRb1-treated microglia increased the proliferation and differentiation of neural precursor cells.

Conclusions

These findings demonstrated that GRb1 alleviated depressive-like behaviors of CMS-exposed male mice mainly through PPARγ-mediated microglial activation and improvement of adult hippocampus neurogenesis.

1. Introduction

Major depressive disorder (MDD), a major public health burden, remains underdiagnosed and undertreated [1]. As a disease involving neuroplasticity dysfunction, MDD is related to chronic neuroinflammation impairment [2]. The imbalance of inflammatory process was observed in rodent models of stress-induced depression, with the increase of pro-inflammatory cytokines interleukin (IL)-1β, IL-6, and IL-18 and the decrease of anti-inflammatory cytokines IL-10, transforming growth factor (TGF)-β, IL-4 [2–4].

Microglia play a key role in immune surveillance of the central nervous system (CNS). Microglia can be activated to show the classical M1 phenotype, associated with up-regulation of pro-inflammatory mediators or the alternative M2 phenotype, associated with up-regulation of anti-inflammatory cytokines [5]. Depending on their phenotypes, activated microglia exert different effects on the differentiation of neural precursor cells (NPCs) *in vivo* and *in vitro*. M1 microglia impair survival and proliferation of NPCs [6], whereas M2 microglia increase the generation of new neurons [7].

There is a close relationship between pathogenesis of depression and the impairment of adult hippocampal neurogenesis. In depression patients, hippocampus atrophy has been reported [8, 9]. In animal models of depression, the depressive-like behaviors are associated with the impairment of adult hippocampal neurogenesis [10]. Neuronal plasticity within the hippocampus is thought to play a significant role in neurobiological responses to stress. Therefore, modulating the switch of microglial phenotypes from neurotoxicity to pro-neurogenesis should be a strategy for treating depression. It has been reported that anti-inflammatory agents such as minocycline inhibited the microglial M1 phenotype [11]. The activation of M2 microglia by anti-inflammatory herbal medicine salvianolic acid B, enhanced neurogenesis and ameliorated depressive-like behaviors [4].

Traditional Chinese medicines are widely used in China and other countries for treatment of mental disorders [12]. Ginseng has been widely applied to treat various conditions in China and other countries over 5000 years, with beneficial effects on immune functions and stress resilience [13, 14]. It was shown high safety of ginseng in clinical prescription [15]. Clinical observations show that ginseng plays significant antidepressant effect [16]. Ginsenoside Rb1 (GRb1), one of main components of Ginseng, has various neuropharmacological effects, including modulating monoamine neurotransmitters, reconstructing neuronal plasticity, regulating the function of hypothalamic-pituitary-adrenal axis, and anti-inflammatory activities [17, 18]. GRb1 exerts significant antidepressant effects in chronic mild stress (CMS)-exposed rodents [19, 20]. However, few studies have focused on the relationship between the antidepressant effects of GRb1 and microglia-mediated neuroinflammatory processes. Already known that GRb1 regulates activation of microglia [21], protecting neurons from inflammatory, oxidative injury and promoting neurogenesis [22].

The peroxisome proliferator-activated receptor gamma (PPARγ), a ligand-activated transcription factor, triggers the expression of anti-inflammatory cytokines that attenuate neurodegeneration [23]. The shifts of M1 microglia to a M2 phenotype with PPARγ agonists such as pioglitazone, down-regulate pro-inflammatory mediators, and up-regulate pro-neurogenic factors in stress-exposed animals [24]. Conversely, PPAR-γ antagonist, GW9662, inhibits the polarization of microglia to M2 phenotype [25]. Here, we tested the hypothesis that GRb1 alleviated depressive-like behaviors mainly through PPARγ-mediated microglial activation and enhancing adult hippocampus neurogenesis in CMS-exposed mice.

2. Material And Methods

2.1 Animals

Adult male C57BL/6J mice 8 weeks old (weighing 18–22 g) were obtained from the Laboratory Animal Center of the Sichuan Academy of Medical Sciences (Chengdu, China). The mice were housed individually under controlled conditions (temperature 23 ± 1.5°C, humidity 65 ± 5%, specific pathogen free, single cage) on a 12 h light/dark cycle (7 PM to 7 AM). Mice were acclimated in 27.5 x 15.5 x 18.5 cm plastic cages with sterile cotton wood sawdust. All experimental procedures were approved by the Ethics Committee of the University of Electronic Science and Technology of China and carried out in strict accordance with the National Institutes of Health Guide for the Care and Use of Laboratory Animals (8th edition, revised 2010).

2.2 Chronic mild stress

Male mice were subjected to CMS as described previously [26]. Briefly, mice were subjected to 1 or 2 kinds of random stressors per day. The stressors included cage tilting (45°, 24 h), reversal of the light-dark cycle (24 h), food or water deprivation (12 h), empty or wet cage (12 h), lights-off (3 h), restraint (2 h), cage shaking (1 h), tail clamping (15 min) and ice water stimulation (5 min).

2.3 Drug administration

GRb1 (purity ≥ 97%, C54H92O23, Cat# P0088) was purchased from Pureone biotechnology company of shanghai. Lipopolysaccharide (LPS, E. Coli, 0127: B8) were purchased from Sigma-Aldrich Chemical Co. (St Louis, MO, USA) and extremely soluble in water. The experiment administered the following treatments once per day (at 16:00 h): saline, GRb1 (20 mg/kg/d, given as a 2 mg/ml solution in 0.9% saline (intragastric administration; Herbpurify, Chengdu, China), or imipramine hydrochloride (IMI, 20 mg/kg/d, intraperitoneally (i.p.); Sigma-Aldrich, Darmstadt, Germany). A subset of stressed animals was pretreated with PPARγ inhibitor GW9662 (1 mg/kg/day in 1% DMSO, i.p., 28 d; Med Chem Express, Monmouth Junction, NJ, USA), then treated 1 h later with GRb1 (control mice were administrated with 1% DMSO solution in 0.9% saline). The doses of GRb1 and IMI were chosen based on previous studies [27, 28].

2.4 Behavioral tests

2.4.1 Locomotor activity test

Locomotor activity of mice was evaluated using a mouse autonomic activity tester (Techman Software-zz6, Chengdu, China) in a quiet environment. In each trial, each mouse was placed in a chamber to acclimatization for 5 min. The numbers of movements and standing were recorded during 10 min test period. After each trial, the apparatus was cleaned using 75% ethyl alcohol.

2.4.2 Sucrose preference test and body weight measurement

The SPT was performed as described previously [4]. Before the test, mice were habituated to consume 1 % sucrose solution for 24 h. In the test, mice were deprived of food and water for 12 h, then provided with two containers of 1% sucrose and the same amount of water for 2 h. Sugar preference (%) was

calculated according to the following formula: Sugar preference (%) = sugar consumption (g) / [sugar consumption (g) + water consumption (g)] × 100%. The SPT and body weight was performed weekly.

2.4.3 Tail suspension test

Each mouse was placed on the end of a rod suspended 30 cm above a tabletop and placed in an individual compartment. The mice were continuously monitored for 6 min using a digital camera. The duration of immobility during 6 min was analyzed.

2.4.4 Forced swim test

The FST was carried out as described previously [29]. Briefly, the glass cylinders (height 21 cm, diameter 12 cm, volume 1000 ml) were filled with tap water (25 ± 2°C). Each mouse was monitored for 6 min using a computer-assisted video camera system (FST-100 Forced Swimming Analysis System, Techman Soft, Chengdu, China). Duration of immobility during the last 4 min was analyzed. FST was performed on week 8 after all other behavioral assays.

2.5 Cell cultures

2.5.1 Primary microglial culture

Primary cultures of microglia from neonatal C57BL/6J mice brain (P0–P3 neonates) were prepared as described previously [30]. Briefly, the entire brain region was dissociated into a single-cell suspension using 0.25% pancreatin (Gibco, California, USA). Neonates were decapitated under sterile conditions, cut off the scalp and skull, removed the brain tissue. And brain tissue was placed in a dish containing cold D-Hank's solution, pH 7.2, without calcium or magnesium (Gibco, California, USA, Cat# C14175500BT). Tissues were enzymatically dissociated into a single-cell suspension using 0.25% pancreatin (Gibco, California, USA), then the mixed glial cells were cultured for 1 week in DMEM/F12 (Gibco, California, USA, Cat# C11330500BT) containing 10% fetal bovine serum (Gibco, California, USA) at 37 °C and 5% CO_2. The isolated microglia were activated with phosphate-buffered saline (PBS, Servicebio, Cat# G4202) or LPS (100 μg/ml; Sigma-Aldrich, Darmstadt, Germany) in the presence or absence of (10, 20, 40) μg/ml GRb1. Some cultures were pretreated for 1 h with 10 μM GW9662, then treated with GRb1 for 24 h, and finally with LPS for 24 h. The collected microglia were transferred to a 6-well plate (2×10^5 cells/cm^2) for subsequent analysis.

2.5.2 NPCs culture

NPCs from C57BL/6J mice (P0–P3, n = 30) were isolated and cultured. Disinfection of infant mice was following the procedure described above in method 2.5.1, and subsequently the hippocampus tissue was dissociated from sagittal brains in ice-cold DMEM/F12, then digested using 0.25% pancreatin (Gibco, California, USA, Cat# 25200056). The digested cells were divided into two parts. One part of the cells (5×10^4 cells/cm^2) was incubated in proliferation medium [high-glucose DMEM/F12, 20 ng/ml epidermal growth factor (Peprotech, Cat# 500-P174G), 20 ng/ml fibroblast growth factor (Peprotech, Cat# 450-33),

40 ng/ml N2 (Gibco, Cat# 17502-048), and 80 ng/ml B27 supplement (Gibco, Cat# 17504-04)]. The second (5×10^4 cells/cm^2) was incubated in differentiation medium (high-glucose DMEM/F12, 40 ng/ml N2, 80 ng/ml B27 supplement, and 10% fetal bovine serum).

2.5.3 Conditioned microglial medium for NPCs culture

Primary microglia were first treated for 24 h with 20 μg/ml GRb1, then with PBS or 100 μg/ml LPS. Some cultures were pretreated for 1 h with 10 μM GW9662, then treated for 24 h with GRb1 and finally treated for 24 h with LPS. These media from microglia were harvested and used as conditioned medium to treat primary NPC cultures that had previously been cultured under the conditions described in the preceding section. Therefore, there were five NPC culture conditions: PBS-conditioned microglial medium (CM), GRb1-conditioned microglial medium (GRb1-CM), LPS-conditioned microglial medium (LPS-CM), LPS + GRb1-conditioned microglial medium (LPS+GRb1-CM), and LPS + GRb1 + GW9662-conditioned microglial medium (LPS+GRb1+GW-CM). NPC proliferation was analyzed after 24 h in the conditioned medium, while NPC differentiation was analyzed after 10 days in the conditioned medium. Areas with the highest cell density were imaged with 20 × on a Zeiss confocal microscope (LSM 800, Germany). Data were analyzed by an investigator blinded to animal treatment.

2.6 RNA extraction and reverse transcription-quantitative PCR (RT-qPCR)

Five mice from each group were randomly selected and sacrificed by decapitation. In accordance with the previous method [31], mice were anesthetized with pentobarbital diluted in 0.9% saline (50 mg/kg, i.p.; R&D Systems, Minneapolis, USA, Cat# 4579/50). Brain tissues were collected after intracardial perfusion with 120 ml cold 0.9% saline solution using a peristaltic pump at 11.5 ml/min. Both hippocampus and cortex were dissected out on ice. Each hemisphere was collected separately for subsequent analyses. Brain tissues were homogenized by the GeneUP Total RNA Mini Kit (Biotechrabbit, Cat# BR0702303). Total RNA (10 ng) was converted to cDNA by reverse transcription with TaKaRa reagent (Takara, Cat# 6210A). The cDNA was stored at -20°C. The following primer pairs were used: β-actin, 5′-CCG TGA AAA GAT GAC CCA GAT C-3′ and 5′-CAC AGC CTG GAT GGC TAC GT-3′; IL-1β, 5′-CCA GCA GGT TAT CAT CAT CAT CC-3′ and 5′-CTC GCA GCA GCA CAT CAA C-3′; tumor necrosis factor (TNF)-α, 5′-TAC TGA ACT TCG GGG TGA TTG GTC C-3′ and 5′-CAG CCT TGT CCC TTG AAG AGA ACC-3′; TGF-β, 5′-GAC CGC AAC AAC GCC ATC TA-3′ and 5′-GGC GTA TCA GTG GGG GTC AG-3′; Arginase (Arg)-1, 5′-AGA CAG CAG AGG AGG TGA AGA G-3′ and 5′-CGA AGC AAG CCA AGG TTA AAG C-3′; PPARγ, 5′-CCC TGG CAA AGC ATT TGT AT-3′ and 5′-CAC CTC TTT GCT CTG CTC CT-3′.

The reaction mixture for RT-qPCR consisted of 1 μl template cDNA, 0.3 μl primer and 5 μl SsoFast EvaGreen Supermix (Bio-Rad, California, USA) in a total volume of 10 μl. Data were reported as fold increase in mRNA levels relative to β-actin.

2.7 Western blotting

Protein extraction, tissue processing, and western blot analysis were based on described method [32]. Protein extraction kit were as followes: Total Protein Extraction kit (Sangon Biotech, Cat# 786-225). Nucleoprotein Extraction Kit (Sangon Biotech, no. c500009). Protein concentration of extracts BCA kit (Beyotime Institute of Biotechnology). Extracts were assayed for total protein using a BCA kit (Beyotime Institute of Biotechnology, Shanghai, China) according to the manufacturer's guidelines. Equal amounts of protein (2 μg/μl, 30 μg) were separated by 12% SDS/PAGE gel electrophoresis, then transferred to nitrocellulose membranes (Servicebio, Cat# G6014-15*15CM). The membranes were covered with 5% skim milk (Servicebio, Cat# G5002) and incubated for 2 h. Then membrane with target protein were incubated overnight at 4°C with rabbit antibodies against PPARγ (1:2,000; IgG, Abcam, 52 KDa, Cat# ab59256, RRID: AB_944767), rabbit antibodies against activated PPARγ (p-PPARγ) (1:500; Thermo Fisher Scientific, 54 KDa, Cat# PA5-36763, RRID: AB_2553712) or GAPDH (1:1,000; 37 KDa, Cat# JM-3777-100, RRID: AB_843142). Lamin B (1:1,000; Wanleibio, 67 KDa, Cat# WL01775). The secondary antibodies goat anti-rabbit IgG (1:10,000; Thermo Fisher Scientific, Cat# 31460, RRID: AB_228341) were incubated for 2 h. Primary and secondary antibodies were all diluted with 5% skimmed milk. Densitometry of protein bands was performed using Image J (version 1.45J; National Institutes of Health, Bethesda, MD, USA).

2.8 Immunofluorescence

To label proliferating cells in the brain, bromodeoxyuridine (BrdU, 50 mg/kg, i.p.; Sigma-Aldrich, Darmstadt, Germany, Cat# B5002) was received 12 h apart. To examine progenitor differentiation in SGZ, animals were injected with a double dose of BrdU and sacrificed 8 weeks after injection. (Fig. 1A). In cell experiment, Brdu was into the medium for 2 h before the test. Mice were anesthetized with pentobarbital sodium (50 mg/kg, i.p.; R&D Systems, Minneapolis, USA, Cat# 4579/50) and perfused transcardially with 120 ml of 0.9% saline using a peristaltic pump, followed by 4% paraformaldehyde with 120 ml. Dissected brains were fixed in 4% paraformaldehyde for 48 h, then dehydrated in 10%, 20%, 30% sucrose solution at 4℃ for 24 h each. For immunostaining against DCX, Iba1 and PPARγ, p-PPARγ. Nuclei were stained with 4',6-diamidin-2-phenylindol (DAPI, Roche, USA, Cat# 10236276001).

The primary antibodies included rat anti-BrdU (1:500; Abcam, Cambridge, UK, Cat# ab6326, RRID: AB_305426,), goat anti-DCX (1:400; goat polyclonal antibody, Santa Cruz, Cat# sc-271390, RRID: AB_10610966), The secondary antibodies (1:1,000; Jackson ImmunoResearch, Pennsylvania, USA) included AffiniPure Donkey Anti-Goat IgG, (Cat# 705-585-003, RRID: AB_2340432), AffiniPure Donkey Anti-Rabbit IgG (Cat# 711-545-152, RRID: AB_2313584), AffiniPure Donkey Anti-Rabbit IgG (Cat# 711-515-152, RRID: AB_2340621). AffiniPure Donkey Anti-Rat IgG, (Cat# 705-585-003, RRID: AB_2340432).

2.9 Morphometry of microglia

Images of hippocampal or cerebral cortical slices (1024 × 1024 pixels) were obtained using a Zeiss confocal microscope (LSM 800, Germany) and the Plan-Apochromat × 63/1.40 NA oil-immersion DIC M27 objective (Zeiss). The mouse brains were sliced into 35 μm thickness slices and were chosen to sample every sixth section based on unbiased counting methods [33]. The brain slice per well was selected sequentially in a 1:6 ratio for a mouse, with each brain slice including the intact hippocampus

and cortex. Microglial density was determined by dividing the number of cells by the total area (mm^3). Microglial morphology was quantified using skeleton analysis method [34]. Images of each slice (1024 × 1024 pixels) were obtained using a Zeiss confocal microscope (LSM 800, Germany). The resulting images were skeletonized using Image J software.

2.10 The quantification of neurogenesis regions

The number of $BrdU^+$ cells and DCX^+ cells in the dentate gyrus (DG) was quantified on the basis of the Cavalieri principle with every sixth section of the hippocampus [35] at 20× objective. In each section, the number of cells was divided by per mm^2 DG in that section [36]. To estimate the total volume of the subregions in the hippocampus, the hippocampal slices were chosen according to the Cavalieri's method, and every sixth section was stained with DAPI antibody at a 40× magnification [37]. We performed the volume measurements of DG and granular cell layer (GCL) in the hippocampal area of 12 sections per animal using the Image J software (version 1.45 J; National Institutes of Health, Bethesda, MD, USA). The volume of subregions was obtained by multiplying the sum of the section areas per animal by 35 μm.

2.11 Statistical analyses

Experiments were performed at least three samples and three times independently. Samples and animals were randomly allocated to experimental groups. The data and statistical analysis comply with the documentation requirements [38]. All experiments were performed in a blinded manner since the measurements could be influenced by personal bias. All data were expressed as mean ± SEM. Statistical analyses were performed using SPSS for Windows ® (version 17; Chicago, USA). In sucrose preference and body weight from week 4 to 8 group, Ctrl and CMS+GRb1 groups at 4^{th} week and 8^{th} week were assessed by three-way repeated measures (ANOVA). CMS and CMS+IMI groups at 4^{th} week and 8^{th} week were analyzed by two-way repeated measures (ANOVA). CMS+GRb1 and CMS+GRb1+GW groups at 4^{th} week and 8^{th} week were performed using two-way repeated measures (ANOVA). A post hoc test was applied only when the F value reached significance and there was no significance in homogeneity of variance. Differences among three or more groups were assessed using one-way or two-way analysis of variance as appropriate, followed by Bonferroni test as post-hoc. The level of confidence was set at 95% ($P < 0.05$), and were done only on datasets of $n \geq 5$. To exclude the misinterpretation of results by the difference in the area of region of interest, the number of proliferating cells in mice, or the total number of cells in each image, normalization of the data was carried out for some analyses in the study.

3. Results

3.1 GRb1 alleviates depressive-like behaviors in male mice exposed to CMS

Previous pharmacokinetics and pharmacodynamics experiments have showed that GRb1 plays a role in a variety of CNS disorders [39]. In the present study, we adopted CMS paradigm, one of the most extensively validated and realistic models of depression [40]. Following exposure to CMS for 8 weeks,

C57BL/6J mice were treated GRb1 at 4th week. The procedure shown in Fig. 1A. We first assessed the locomotor ability of mice. In spontaneous activity, there was no statistically difference in activity level or standing time among groups, indicating that the drug treatment had no effect on motor ability (Fig. 1B). The weight gain was inhibited by CMS exposure at 4th and 8th week. The CMS-induced reduction of weight gain was attenuated by GRb1 and IMI at week 8 (Fig. 1C). The FST and TST were performed to test the desperate behaviors of mice. Chronic stress caused mice to remain immobile for longer periods, whereas the GRb1-treated and IMI-treated mice displayed decreased immobility time in both TST and FST, similar to that of Ctrl mice (Fig. 1D–1E). The sucrose preference test is commonly used to evaluate anhedonia in animals. The CMS groups showed reduction in sucrose consumption between week 4 and 8. Both GRb1 and IMI-treated mice displayed increase the sucrose consumption compared with CMS group (Fig. 1F). The obtained results indicated that GRb1 was able to recover depressive-like behaviors in CMS-exposed mice.

3.2 GRb1 promotes microglial M2-polarization in the hippocampus and cortex.

Depression as a microglial disease [41], we next explored whether GRb1 could activated microglial polarization. The microglial morphological property using immunofluorescence labeling. Iba1 as microglia-specific marker (Fig. 2A–2B). Results showed that CMS significantly increased the density of $Iba1^+$ cells in hippocampus and cortex, while treatment with GRb1 significantly prevented the increase in cell density of CMS mice (Fig. 2C). When microglia are activated, they switch from ramified to amoeboid morphology. Correspondingly, hippocampal microglia in CMS animals had larger and bigger soma, fewer and shorter processes than Ctrl group. GRb1 treatment of CMS-exposed mice reduced the cell area (Fig. 2D), increased the number and the total length of microglia processes (Fig. 2E–2F). Whereas cortical microglia had shorter processes in CMS animals than Ctrl animals, and GRb1 treatment increased the cell area, the number of processes in cortex (Fig. 2D–2F). Polarized microglia also are distinguished by their expression profiles of signature surface markers. Stress up-regulated the pro-inflammatory (M1 microglia) markers TNF-α and IL-1β in hippocampus and cortex, while down-regulated M2 microglial markers TGF-β and Arg-1. GRb1 inhibited these changes (Fig. 2G–2J). These results indicated that GRb1 activated M2-like polarized microglia.

3.3 GRb1 rescues neurogenesis impairment in hippocampus

Adult hippocampal neurogenesis as a potential candidate mechanism for the etiology of depression [42]. We then examined whether GRb1 was involved in neurogenesis. Proliferative cells were labeled with BrdU, and newborn neurons were labeled with DCX (Fig. 3A). Chronic stress decreased the mRNA level of DCX, which was increase by GRb1 (Fig. 3B). The immunofluorescence results indicated that CMS also decreased the number of $BrdU^+$ cells in DG, which was restored by GRb1 (Fig. 3C). Here, at 8 weeks post-BrdU injection, chronic stress significantly reduced the number of DCX^+ cells and the “differentiation ratio” in DG, which was significantly increased in GRb1 group (Fig. 3D–3E). In addition, in order to determine whether the effects of GRb1administration on hippocampus volume, we performed analysis of volume in DG and GCL. The results revealed that GRb1 reversed the reduction the volume of DG and GCL in CMS

group (Fig. 3F–3H). The CMS group also showed a tendency to cause thinning of GCL, which GRb1 reversed (Fig. 3I). In contrast, no alterations were found in administering GRb1 in the absence of CMS in neurogenesis of hippocampus.

3.4 GRb1 activates PPARγ expression in CMS-induce depression model

Activation of the nuclear receptor PPARγ prevents microglial activation, and PPARγ antagonist aggravates microglia-regulated neuroinflammation [43]. We therefore hypothesized that GRb1 treatment could mediated PPARγ activation. We performed GW9662 as PPARγ effective inhibitors. CMS down-regulated PPARγ mRNA in hippocampus, which GRb1 up-regulated PPARγ mRNA in hippocampus (Fig. 4A). GRb1 had slight downward trend of PPARγ mRNA levels in cortex of CMS group. (Fig. 4B). We further verified the PPARγ expression or p-PPARγ expression at the protein level (Fig. 4C–4D). Western blotting showed that in hippocampus, the CMS significantly reduced levels of PPARγ and p-PPARγ in total protein and nuclear protein. The levels of p-PPARγ in nuclei were also decreased in CMS-treated mice, GRb1 inhibited CMS-induced reduction of PPARγ and p-PPARγ; In cortex, Reduction of PPARγ protein in CMS group compared with control group (Fig. 4E–4J). Whether this function was reversed by PPARγ inhibitor GW9662. Indeed, the above PPARγ expression were significantly reversed by PPARγ inhibitor GW9662 in hippocampus. Administering GRb1 alone had no effect on PPARγ expression at mRNA or protein level.

3.5 PPARγ activation mediates effects of GRb1-induced microglia

We first assessed whether the effect of antidepressant of GRb1-induced microglia was mediated by PPARγ activation. Mice were treated with GW9662 treatment, blocking the PPARγ pathway, before GRb1 administration on CMS condition. We found that the GW9662 treatment notably blocked the effects of antidepressant of GRb1 on the decrease of body weight, the increase of the immobility time in FST, the reduction of sucrose consumption, without affecting autonomic activity. The GW9662 administration also caused similar trends in both weight change and sucrose preference as those in the CMS group at week 4 and week 8 (Fig. 1B–1F). We then examined the interception of GW9662 administration on GRb1-induced microglial activation. Indeed, the GW9662 administration weakened the effects of GRb1 on $Iba1^+$ cell number (Fig. 2C) and microglial morphology in the hippocampus (Fig. 2E–2F). In cortex, the GW9662 treatment blocked only the effects of GRb1 on $Iba1^+$ cell number in CMS-exposed mice (Fig. 2C). We also found that GW9662 treatment dramatically reversed GRb1-induced down-regulation of M1 markers and up-regulation of M2 markers in hippocampus (Fig. 2G–2H). Similar results were observed in cortex, except that GW9662 treatment did not affect GRb1-induced down-regulation of TNF-α (Fig. 2I–2J). We then examined PPARγ inhibitor in neurogenesis in CMS mice. The GW9662 treatment dramatically decreases in the level of DCX mRNA in compared with GRb1 + CMS group (Fig. 3B), the GW9662 treatment reduced the neurogenesis (Fig. 3C–3I). The results provided evidence that GRb1 activated M2 microglia and promoted neurogenesis dependent on PPARγ pathway.

3.6 PPARγ activation mediates effects of GRb1-induced microglia *in vitro*

Primary cultures of microglia were stimulated by LPS in the presence or absence of GRb1, with or without GW9662. To maximize drug effectiveness *in vitro*, 20 μg/ml of GRb1 was chosen to be used in the following experiments to determine the regulatory effect of GRb1 on the activation of microglia and neurogenesis (Fig. S1). Cultures were analyzed by immunofluorescence to assess microglial morphology and PPARγ expression (Fig. 5A). GRb1 increased the PPARγ expression in LPS group, which GW9662 reversed the increase (Fig. 5B). GRb1 up-regulated the PPARγ expression in LPS treatment. LPS-treated primary microglia exhibited round soma and developed longer processes. GRb1 pretreatment inhibited LPS-induced microglial activation, decreasing the $Iba1^+$ cell area and length of processes, and this change was significantly suppressed by GW9662 (Fig. 5C–5D). To correlate these effects with neurogenesis, we treated NPCs with some stimuli (Fig. 5E). Proliferative cells were labeled with BrdU, and newborn neurons were labeled with DCX (Fig. 5F). GRb1 increased the ratio of $BrdU^+$ to $DAPI^+$ NPCs, which GW9662 did significantly reduced (Fig. 5G). The GRb1 treatment increased the ratio of DCX^+ to $DAPI^+$ cells (Fig. 5I). The GRb1 alone showed no significant effects on the ratio of BrdU + to DAPI + and DCX + to DAPI + cells NPCs.

Next we asked whether the effects of GRb1 on neurogenesis were mediated by microglia. Primary cultures of NPCs were incubated in conditioned medium from microglia. Conditioned medium from microglia stimulated with LPS reduced the ratios of $BrdU^+$ to $DAPI^+$ cells and DCX^+ to $DAPI^+$ cells, and GRb1-CM increase the ratios, whereas the effect was inhibited by pretreated with GW9662 (Fig. 5H–5J). These results indicated that GRb1-mediated M2 microglia stimulated neurogenesis dependent on PPARγ activation *in vitro*.

4. Discussion

GRb1 shows antidepressant effects in rodent models of stress-induced depression. Our present study discloses that GRb1 alleviates depressive-like behaviors by regulating inflammatory cytokines in hippocampus and cortex of CMS-exposed mice. Moreover, the results revealed that GRb1 treatment shifted microglia to M2 phenotype and stimulating neurogenesis in hippocampus. The data from *in vivo* and *in vitro* both indicated that GRb1-induced shift in microglial phenotype was dependent on PPARγ pathway. These findings provided first evidence that GRb1 induced a pro-neurogenic microglial phenotype via PPARγ activation in hippocampus of CMS-exposed mice.

In order to prove the antidepressant effect of GRb1, we conducted *in vivo* studies using male mice exposed to CMS. CMS model is widely used to investigate the underlying mechanism animal lines of depression [45]. The most obvious feature of CMS is anhedonia, that is a decreased preference for sugar water. Another feature is an extinction-like inhibitory learning behavior, that is longer immobility time in both FST and TST. GRb1 and IMI administration can reverse the effects of anhedonia and desperate behaviors. Since no alterations in the spontaneous locomotor activity were found, the results indicated that antidepressant-like activity of GRb1 exerted antidepressant effects in CMS depression model, not affect the locomotor ability. Sex as an important biological variable from basic and preclinical research

[46]. It has been previously reported that GRb1 ameliorated the depressive-like behaviors in ovariectomized or menopausal female mice. [47, 48], indicating that the potential function of the sex hormone effects of GRb1 on depression would be achieved further investigation in the future studies.

Accumulating evidence supports an association between depression and inflammatory processes [49]. As a primary source of inflammatory molecules in the CNS, microglia show a spectrum of polarization phenotypes responsible for balance of pro- and anti-inflammatory mediators [50]. Chronic stress activates hippocampal microglia, microglia tended to show an M1 phenotype, causing soma enlargement, shortening and thickening of processes. Activated microglia were also characterized by increasing expression of TNF-α and IL-1β and decreasing expression of the M2 markers TGF-β and Arg-1. GRb1 treatment *in vivo* significantly reduced the area of hippocampal $Iba1^+$ cells and increased the number and total length of microglial processes. Meanwhile, GRb1 decreased the expression of M1 markers and increased the expression of M2 markers. These results suggested that GRb1 shifted the phenotype of microglia from M1 to M2 polarization in CMS-exposed mice. Since there were interactions between various cell types in brain, the direct effect of GRb1 on microglial morphology was further tested on primary microglia. The result showed that GRb1 directly prevented LPS-induced effects on microglial activation, consistent with the effects of GRb1 *in vivo*.

Impairment of hippocampal neurogenesis has been associated with inflammation-mediated depressive-like symptoms. Neurogenesis occurs predominantly in the SGZ of hippocampus and subependymal ventricular zone [51]. Our results showed that GRb1 significantly increased the number of $BrdU^+$ and DCX^+ cells, as well as the differentiation ratio in SGZ. Several studies performed using magnetic resonance imaging showed similar total brain volume but smaller hippocampal volume in patients with depression than in controls [52]. Post mortem analysis of depressed patients has shown a reduction in hippocampal volume [53]. Consistent with these results, our data showed that stess decreased the volume of DG and GCL, while long-term treatment with GRb1 significant amelioration of neuronal structural changes. Previous studies have reported that persistent production of pro-inflammatory cytokines is detrimental to neurogenesis [54]. Based on our observation that a shift of microglial phenotypes from M1 to M2, pretreatment of GRb1 reversed chronic stress-induced the impairment in hippocampal neurogenesis. we speculated that GRb1-induced M2 microglia played a phenotype-associated neurogenic role.

We next analyzed the role of microglia on neurogenesis *in vitro* using conditioned media. LPS-CM reduced the proliferation and differentiation of NPCs, while GRb1 + LPS-CM promoted the proliferation and differentiation of NPCs. GRb1 appeared to play a subtle neurogenic effect on immune-stimulated NPCs, promoting their proliferation but not differentiation. Consistent with our results, M1 microglia promoted astrocytogenesis, while M2 microglia supported neurogenesis *in vitro* [55]. Liu et al. [56] reported that GRb1 increased survival of newborn neurons and didn't influence NPCs proliferation in non-stressed rat. Our different findings of GRb1 on NPCs proliferation may come from different animal models, which remain to be confirmed. These *in vivo* and *in vitro* results implied that GRb1 enhanced

neurogenesis via switching microglial phenotype from M1 to M2, contributing to neurogenesis in CMS-exposed mice.

Mounting evidence has been presented demonstrating that GRb1 has anti-inflammatory and neuroprotective effects. Ying et al. [57] suggested that GRb1 exerted antidepressant effects via multiple cellular and molecular pathways. PPARγ is a ligand-activated transcription factor that regulates the expression of inflammatory cytokines and microglial phenotypes [58]. We thus reasoned that GRb1-activated microglia may be related to PPARγ pathway. As expected, our study showed that GRb1 up-regulated PPARγ expression and enhanced PPARγ activation in the hippocampus of CMS-treated mice. GRb1 also altered phenotype of microglia transition from M1 to M2, increasing neurogenesis in hippocampus. As an approach to corroborate these findings, we used PPARγ antagonist GW9662 to intercept microglial activation. The results indicated that the GW9662 treatment strongly prevent GRb1-induced microglial activation *in vivo* and *in vitro*. Furthermore, the culture NPCs using conditioned medium from microglia showed that GRb1 enhanced the proliferation and differentiation of NPCs via PPARγ-mediated microglia *in vitro*. The results of this experiment showed that inhibition of PPARγ activation produced a significant dysregulation in neurogenesis mediated by microglia. Our experiments highlighted the functional role of microglia as components of a neurogenic niche in the brain, and implicated the role of PPARγ activation in NPCs proliferation and differentiation.

5. Conclusion

Our study provides strong *in vivo* and *in vitro* evidence that GRb1 exerts antidepressant effects by activating PPARγ to shift microglia towards an anti-inflammatory, pro-neurogenic phenotype. Our findings may shed light on the potential contribution of GRb1-treated microglia to promote neurogenesis as a therapeutic strategy against MDD.

Abbreviations

Arg, Arginase; BrdU, Bromodeoxyuridine; CMS, chronic mild stress; CNS, central nervous system; DAPI, 4’,6-diamidin-2-phenylindol; DG, dentate gyrus; FST, force swimming test; GCL, granular cell layer; GRb1, Ginsenoside Rb1; IL, interleukin; IMI, imipramine; LAT, locomotor activity test; LPS, lipopolysaccharide; MDD, Major depressive disorder; NPC, neural precursor cell; OFT, open field test; PPARγ, peroxisome proliferator-activated receptor gamma; RT-qPCR, reverse transcription-quantitative PCR; SGZ, subgranular zone; SPT, sucrose preference test; TGF, transforming growth factor; TNF, tumor necrosis factor; TST, tail suspension test.

Declarations

Acknowledgements

We are grateful to Prof. Zujun Yang for providing materials and assistance with immunohistochemistry, and to A. Chapin Rodríguez for help in revising the manuscript.

Authors' contributions

Author's contributions: L.Z. designed the study, performed experiments and wrote the paper. M.T., Q. Z. and X.X. designed and performed statistical analysis of animal behavior experiments. N.H. and H.H. performed experiments and analyzed quantitative PCR and western blot data. G.L. and S.H. performed experiments and analyzed immunofluorescence data. C.P., Y.X. and Z.Y. designed the study and revised the paper.

Funding

This work was supported by the National Natural Science Foundation of China (81701308), Sichuan Science and Technology Program (2020YJ0225, 2019JDPT0010), the Open Research Fund, Key Laboratory of Systematic Research, Distinctive Chinese Medicine Resources in Southwest China (2018003), and CAS Key Laboratory of Mental Health, Institute of Psychology (KLMH2019K04).

Availability of data and materials

All data generated and materials supporting the conclusion of the study are included within the article and its supplementary information files.

Competing interests

All authors declare that there are no conflicts of interest.

Consent for publication

Not applicable

Ethics approval and consent to participate

All animals care and experimental procedures were approved by the Ethics Committee of the University of Electronic Science and Technology of China and carried out in strict accordance with the National Institutes of Health Guide for the Care and Use of Laboratory Animals.

References

1 Smith K. Mental health: a world of depression. Nature 2014; 515: 181.

2 You Z, Luo C, Zhang W, Chen Y, He J, Zhao Q, Zuo R, Wu YH. Pro- and anti-inflammatory cytokines expression in rat's brain and spleen exposed to chronic mild stress: involvement in depression. Behav Brain Res 2011; 225: 135-41.

3 Liu YM, Shen JD, Xu LP, Li HB, Li YC, Yi LT. Ferulic acid inhibits neuro-inflammation in mice exposed to chronic unpredictable mild stress. Int Immunopharmacol 2017; 45: 128-34.

4 Zhang J, Xie X, Tang M, Zhang J, Zhang B, Zhao Q, Han Y, Yan W, Peng C, You ZL. Salvianolic acid B promotes microglial M2-polarization and rescues neurogenesis in stress-exposed mice. Brain Behav Immun 2017; 66: 111-24.

5 Zhang L, Zhang J, You Z. Switching of the Microglial Activation Phenotype Is a Possible Treatment for Depression Disorder. Front Cell Neurosci 2018; 12: 306.

6 Ulrike VS, Jessica FL, Monika R, Rebecca R, Stefan B, Judith K, Reinert N, Bach A, Fink GR, Schroeter M, et al. The plasticity of primary microglia and their multifaceted effects on endogenous neural stem cells *in vitro* and *in vivo*. J Neuroinflammation 2018; 15: 226.

7 Butovsky O, Ziv Y, Schwartz A, Landa G, Talpalar AE, Pluchino S, Martino G, Schwartz M. Microglia activated by IL-4 or IFN-gamma differentially induce neurogenesis and oligodendrogenesis from adult stem/progenitor cells. Mol Cell Neurosci 2006; 31: 149-60.

8 Chana G, Landau S, Beasley C, Everall IP, Cotter D. Two-dimensional assessment of cytoarchitecture in the anterior cingulate cortex in major depressive disorder, bipolar disorder, and schizophrenia: evidence for decreased neuronal somal size and increased neuronal density. Biol Psychiatry 2003; 53: 1086-98.

9 Valdés-Tovar M, Estrada-Reyes R, Solís-Chagoyán H, Argueta J, Dorantes-Barrón AM, Quero-Chávez D, Cruz-Garduño R, Cercós MG, Trueta C, Oikawa-Sala J, et al. Circadian modulation of neuroplasticity by melatonin: a target in the treatment of depression. Br J Pharmacol 2018; 175: 3200-8.

10 Liang M, Zhong H, Rong J, Li Y, Zhu C, Zhou L, Zhou R. Postnatal Lipopolysaccharide Exposure Impairs Adult Neurogenesis and Causes Depression-like Behaviors Through Astrocytes Activation Triggering GABAA Receptor Downregulation. J Neuroscience 2019; 422: 21-31.

11 Han Y, Zhang L, Wang Q, Zhang D, Zhao Q, Zhang J, Xie L, Liu G, You Z. Minocycline inhibits microglial activation and alleviates depressive-like behaviors in male adolescent mice subjected to maternal separation. Psychoneuroendocrinology. 2019;107:37-45.

12 Jiang Y, David B, Tu P, Barbin Y. Recent analytical approaches in quality control of traditional Chinese medicines—A review. J Analytica Chimica Acta 2010; 657: 9-18.

13 Ratan ZA, Youn SH, Kwak YS, Han CK, Haidere MF, Kim JK, Min H, Jung YJ, Hosseinzadeh H et al., Adaptogenic effects of Panax ginseng on modulation of immune functions. J Ginseng Res. 2021;45(1):32-40.

14 Nair R., Sellaturay S., Sriprasad S. The history of ginseng in the management of erectile dysfunction in ancient China (3500-2600 BCE) Indian J Urol. 2012;28:15–20.

15 Shergis JL, Thien F, Worsnop CJ, Lin L, Zhang AL, Wu L, Yuanbin ChenYB, Xu YJ, Langton D, Costa CD, et al. 12-month randomised controlled trial of ginseng extract for moderate COPD. Thorax 2019; 74: 539-45.

16 Jeong HG, Ko YH, Oh SY, Han C, Kim T, Joe SH. Effect of Korean Red Ginseng as an adjuvant treatment for women with residual symptoms of major depression. Asia Pac Psychiatry 2015; 7: 330–6.

17 Ahmed T, Raza SH, Maryam A, Setzer WN. Ginsenoside Rb1 as a neuroprotective agent: A review. Brain Res Bull 2016; 125: 30-43.

18 Guo Y, Xie J, Zhang L, Yang L, Ma J, Bai Y, Ma W, Wang L, Yu H, Zeng Y et al., Ginsenoside Rb1 exerts antidepressant-like effects via suppression inflammation and activation of AKT pathway. Neurosci Lett. 2021 Jan 23;744:135561.

19 Wang GL, He ZM, Zhu HY, Gao YG, Zhao Y, Yang H, Zhang LX. Involvement of serotonergic, noradrenergic and dopaminergic systems in the antidepressant-like effect of ginsenoside Rb1, a major active ingredient of Panax ginseng C.A. Meyer. J Ethnopharmacol 2017; 204: 118.

20 Wang GL, Wang YP, Zheng JY, Zhang LX. Monoaminergic and aminoacidergic receptors are involved in the antidepressant-like effect of ginsenoside Rb1 in mouse hippocampus (CA3) and prefrontal cortex. Brain Res 2018; 1699: 44-53.

21 Wang D, Zhao S, Pan J, Wang Z, Li Y, Xu X, Yang J, Zhang X, Wang Y, Liu M. Ginsenoside Rb1 attenuates microglia activation to improve spinal cord injury via microRNA-130b-5p/TLR4/NF-κB axis. J Cell Physiol 2021;236(3):2144-2155.

22 Li DW, Zhou FZ, Sun XC, Li SC, Yang JB, Sun HH, Wang AH. Ginsenoside Rb1 protects dopaminergic neurons from inflammatory injury induced by intranigral lipopolysaccharide injection. Neural Regen Res. 2019;14(10):1814-1822.

23 Dandan Z, Lei J, Youguo C. TSPO Modulates IL-4-Induced Microglia/Macrophage M2 Polarization via PPAR-γ Pathway. J Mol Neurosci 2020; 70: 542-9.

24 Mandrekar-Colucci S, Karlo JC, Landreth GE. Mechanisms Underlying the Rapid Peroxisome Proliferator-Activated Receptor-γ-Mediated Amyloid Clearance and Reversal of Cognitive Deficits in a Murine Model of Alzheimer's Disease. J Neuroscience 2012; 32: 10117-28.

25 Wen L, You W, Wang H, Meng Y, Feng J. Polarization of Microglia to the M2 Phenotype in a Peroxisome Proliferator-Activated Receptor Gamma-Dependent Manner Attenuates Axonal Injury Induced by Traumatic Brain Injury in Mice. J Neurotrauma 2018; 35: 2330-40.

26 Joung JY, Song JG, Kim HW, Oh NS. Protective Effects of Milk Casein on the Brain Function and Behavior in a Mouse Model of Chronic Stress. J Agric Food Chem. 2021;69(6):1936-1941.

27 Zhang JQ, Wu XH, Feng Y, Xie XF, Fan YH, Yan S, Zhao QY, Peng C, You ZL. Salvianolic acid B ameliorates depressive-like behaviors in chronic mild stress-treated mice: involvement of the neuroinflammatory pathway. Acta Pharmacol Sin 2016; 37: 1141-53.

28 Wang G, Lei C, Tian Y, Wang Y, Zhang R. Rb1, the Primary Active Ingredient in Panax ginseng C.A. Meyer, Exerts Antidepressant-Like Effects via the BDNF–Trkb–CREB Pathway. Front Pharmacol 2019; 10: 1034.

29 Yankelevitch-Yahav R, Franko M, Huly A, Doron RJ. The Forced Swim Test as a Model of Depressive-like Behavior. J Vis Exp 2015;(97):52587.

30 Newell EA, Exo JL, Verrier JD, Jackson TC, Gillespie DG, Janesko-Feldman K, Kochanek PM, Jackson EK. 2',3'-cAMP, 3'-AMP, 2'-AMP and Adenosine Inhibit TNF-α and CXCL10 Production From Activated Primary Murine Microglia via A2A Receptors. Brain Res. 2015;1594:27-35.

31 Roszkowski M, Bohacek J. Stress does not increase blood–brain barrier permeability in mice. J Cereb Blood Flow Metab 2016; 36.

32 Wang HY, Huang M, Wang W, Zhang Y, Ma X, Luo L, Xu XT, Xu L, Shi HB, Xu YM, et al. Microglial TLR4-induced TAK1 phosphorylation and NLRP3 activation mediates neuroinflammation and contributes to chronic morphine-induced antinociceptive tolerance. Pharmacol Res 2021: 105482.

33 Encinas JM, Enikolopov G. Identifying and quantitating neural stem and progenitor cells in the adult brain. Methods Cell Biol 2008; 85: 243-72.

34 Young K, Morrison H. Quantifying Microglia Morphology from Photomicrographs of Immunohistochemistry Prepared Tissue Using ImageJ. J Vis Exp 2018; 136: 57648.

35 Khazipov R, Zaynutdinova D, Ogievetsky E, Valeeva G, Mitrukhina O, Manent J-B, Represa A. Atlas of the Postnatal Rat Brain in Stereotaxic Coordinates. Front Neuroanat 2015; 9: 161.

36 Novati A, Hulshof HJ, Koolhaas JM, Lucassen PJ, Meerlo P. Chronic sleep restriction causes a decrease in hippocampal volume in adolescent rats, which is not explained by changes in glucocorticoid levels or neurogenesis. Neuroscience 2011; 190: 145-55.

37 Gundersen HJ, Jensen EB. The efficiency of systematic sampling in stereology and its prediction. J Microsc. 1987;147(Pt 3):229-63.

38 Curtis MJ, Alexander S, Cirino G, Docherty JR, George CH, Giembycz MA, Hoyer D, Insel PA, Izzo AA, Ji Y, et al. Experimental design and analysis and their reporting II: updated and simplified guidance for authors and peer reviewers. Br J Pharmacol 2018; 175: 987-93.

39 Kennedy DO, Scholey AB. Ginseng: potential for the enhancement of cognitive performance and mood. Pharmacol Biochem Behav 2003; 75: 687-700.

40 Czéh B, Fuchs E, Wiborg O, Simon M. Animal models of major depression and their clinical implications. Prog Neuropsychopharmacol Biol Psychiatry 2015; 64: 293-310.

41 Yirmiya R, Rimmerman N, Reshef R. Depression as a microglial disease. Trends Neurosci 2015;38(10):637-658.

42 Sahay A, Hen R. Adult hippocampal neurogenesis in depression. Nat Neurosci. 2007;10(9):1110-5.

43 Zhao Q, Wu X, Yan S, Xie X, Fan Y, Zhang J, Peng C, You ZL. The antidepressant-like effects of pioglitazone in a chronic mild stress mouse model are associated with PPARγ-mediated alteration of microglial activation phenotypes. J Neuroinflammation 2016; 13: 259.

44 Gao H, Kang N, Hu C, Zhang Z, Yang S. Ginsenoside Rb1 exerts anti-inflammatory effects *in vitro* and *in vivo* by modulating Toll-like Receptor 4 dimerization and NF-kB/MAPKs signaling pathways. Phytomedicine 2020; 69: 153197.

45 Hao Y, Ge H, Sun M, Gao Y. Selecting an Appropriate Animal Model of Depression. Int J Mol Sci. 2019;20(19):4827.

46 Lee SK. Sex as an important biological variable in biomedical research. BMB Rep. 2018;51(4):167-173.

47 Hao K, Gong P, Sun S, Hao H, Wang G, Dai Y, Liang Y, Xie L, Li FY. Beneficial estrogen-like effects of ginsenoside Rb1, an active component of Panax ginseng, on neural 5-HT disposition and behavioral tasks in ovariectomized mice. Eur J Pharmacol 2011; 659: 15-25.

48 Yamada N, Araki H, Yoshimura H. Identification of antidepressant-like ingredients in ginseng root (Panax ginseng C.A. Meyer) using a menopausal depressive-like state in female mice: participation of 5-HT2A receptors. Psychopharmacology (Berl) 2011; 216: 589-99.

49 Khler O, Krogh J, Mors O, Benros ME. Inflammation in Depression and the Potential for Anti-Inflammatory Treatment. Curr Neuropharmacol 2015; 14: 732-42.

50 Wang Y, Han Q, Gong W, Pan D, Wang L, Hu W, Yang M, Li B, Yu J, Liu Q. Microglial activation mediates chronic mild stress-induced depressive- and anxiety-like behavior in adult rats. J Neuroinflammation. 2018;15(1):21.

51 Kaoru S. Effects of Microglia on Neurogenesis. Glia 2015; 63: 1394-405.

52 Campbell S, Marriott M, Nahmias C, Macqueen GM. Lower hippocampal volume in patients suffering from depression: a meta-analysis. Am J Psychiatry 2004; 161: 598-607.

53 Stockmeier CA, Mahajan GJ, Konick LC, Overholser JC, Jurjus GJ, Meltzer HY, Uylings Harry B M, Friedman L, Rajkowska G. Cellular changes in the postmortem hippocampus in major depression. Biological Psychiatry 2004; 56: 640-50.

54 Ekdahl CT, Kokaia Z, Lindvall O. Brain inflammation and adult neurogenesis: the dual role of microglia. Neuroscience 2009; 158: 1021-9.

55 Vay SU, Vay SU, Flitsch LJ, Rabenstein M, Rogall R, Blaschke S, Kleinhaus J, Reinert N, Bach A, Fink GR, Schroeter M, Rueger MA. The plasticity of primary microglia and their multifaceted effects on endogenous neural stem cells *in vitro* and *in vivo*. J Neuroinflammation. 2018;15(1):226.

56 Liu L, Hoang-Gia T, Wu H, Lee MR, Gu L, Wang C, Yun BS, Wang QJ, Ye SQ, Sung CK. Ginsenoside Rb1 improves spatial learning and memory by regulation of cell genesis in the hippocampal subregions of rats. Brain Research 2011; 1382: 147-54.

57 Guo Y, Xie J, Zhang L, Yang L, Ma J, Bai Y, Ma WJ, Wang L, Yu HF, Zeng YQ, et al. Ginsenoside Rb1 exerts antidepressant-like effects via suppression inflammation and activation of AKT pathway. Neurosci Lett 2020; 744: 135561.

58 Guo M, Li C, Lei Y, Xu S, Zhao D, Lu XY. Role of the adipose PPARγ-adiponectin axis in susceptibility to stress and depression/anxiety-related behaviors. Mol Psychiatry 2016; 22: 1056-68.

Tables

Table 1 The F value and P value in multiple comparisons of figure 1

figure	group	F or T	P	N
Figure 1B-1	CMS vs. Ctrl		0.0970	
	GRb1 vs. Ctrl	4.612	0.1135	12
	CMS+GRb1 vs. CMS		0.9942	
	CMS+IMI vs. CMS		0.2171	
	CMS+IMI vs. CMS+GRb1	1.903	0.0702	
	CMS+GRb1+GW vs. CMS+GRb1	1.734	0.0968	12
Figure 1B-2	CMS vs. Ctrl		0.2054	
	GRb1 vs. Ctrl	1.411	0.6570	12
	CMS+ GRb1 vs. CMS		0.6361	
	CMS+IMI vs. CMS		0.9489	
	CMS+ IMI vs. CMS+GRb1	0.076	0.9399	
	CMS+GRb1+GW vs. CMS+GRb1	0.336	0.7401	12
Figure 1C-1	Treatment vs Basal (Ctrl)		0.0020	
	Treatment vs Basal (GRb1)		0.0010	
	Treatment vs Basal (CMS)		0.0750	
	Treatment vs Basal (CMS+GRb1)	14.211	< 0.0001	12
	Treatment vs Basal (CMS+IMI)		< 0.0001	
	Treatment vs Basal (CMS+GRb1+GW)		0.0960	
	Ctrl vs CMS (Basal)		< 0.0001	
	CMS+GRb1 vs CMS (treatment)		< 0.0001	
	CMS+IMI vs CMS (treatment)	4.540	0.0631	12
	CMS+GRb1+GW vs. CMS+GRb1 (treatment)		< 0.0001	
	CMS vs. Ctrl		0.0343	

Figure 1C-2	GRb1 vs. Ctrl	4.636	0.9032	12
	CMS+ GRb1 vs. CMS		0.0035	
	CMS+IMI vs. CMS		0.1519	
	CMS+ IMI vs. CMS+GRb1	0.472	0.6416	
	CMS+GRb1+GW vs. CMS+GRb1		0.0003	12
		4.255		
Figure 1D	CMS vs. Ctrl		0.0002	
	GRb1 vs. Ctrl	43.820	>0.9999	12
	CMS+ GRb1 vs. CMS		< 0.0001	
	CMS+IMI vs. CMS		0.0006	
	CMS+ IMI vs. CMS+GRb1	1.097	0.2846	
	CMS+GRb1+GW vs. CMS+GRb1		0.0001	12
		4.721		
Figure 1E	CMS vs. Ctrl		< 0.0001	
	GRb1 vs. Ctrl	6.458	0.6054	12
	CMS+GRb1 vs. CMS		< 0.0001	
	CMS+IMI vs. CMS		0.0001	
	CMS+ IMI vs. CMS+GRb1	0.513	0.6127	
	CMS+GRb1+GW vs. CMS+GRb1		0.0003	12
		4.228		

	Treatment vs Basal (Ctrl)		0.0720	
	Treatment vs Basal (GRb1)		0.1241	
Figure 1F-1	Treatment vs Basal (CMS)		0.4190	
	Treatment vs Basal (CMS+GRb1)	7.804	< 0.0001	12
	Treatment vs Basal (CMS+IMI)		< 0.0001	
	Treatment vs Basal (CMS+GRb1+GW)		0.4515	
	Ctrl vs CMS (Basal)		< 0.0001	
	CMS+GRb1 vs CMS (treatment)		< 0.0001	
	CMS+IMI vs CMS (treatment)	18.730	< 0.0001	12
	CMS+GRb1+GW vs. CMS+GRb1 (treatment)		< 0.0001	
Figure 1F-2	CMS vs. Ctrl		< 0.0001	
	GRb1 vs. Ctrl	33.920	0.1233	12
	CMS+ GRb1 vs. CMS		< 0.0001	
	CMS+IMI vs. CMS		< 0.0001	
	CMS+ IMI vs. CMS+GRb1	0.809	0.4287	
	CMS+GRb1+GW vs. CMS+GRb1	3.135	0.0057	12

Table 2The F value and P value in multiple comparisons of figure 2

figure	group	F or T	P	N
Figure 2C-h	CMS vs. Ctrl		< 0.0001	
	GRb1 vs. Ctrl	33.920	0.1233	6
	CMS+GRb1 vs. CMS		< 0.0001	
	CMS+GRb1+GW vs. CMS+GRb1	8.648	< 0.0001	6
Figure 2C-c	CMS vs. Ctrl		0.0002	
	GRb1 vs. Ctrl	7.923	0.2627	6
	CMS+ GRb1 vs. CMS		0.0004	
	CMS+GRb1+GW vs. CMS+GRb1	2.444	0.0193	6
Figure 2D-h	CMS vs. Ctrl		0.0207	
	GRb1 vs. Ctrl	2.347	0.6339	5
	CMS+ GRb1 vs. CMS		0.0155	
	CMS+GRb1+GW vs. CMS+GRb1	3.191	0.0057	6
Figure 2D-c	CMS vs. Ctrl		0.2343	
	GRb1 vs. Ctrl	8.559	0.2388	6
	CMS+GRb1 vs. CMS		0.0441	
	CMS+GRb1+GW vs. CMS+GRb1	2.107	0.0682	
Figure 2E-h	CMS vs. Ctrl		0.0006	
	GRb1 vs. Ctrl	5.422	0.1039	6
	CMS+GRb1 vs. CMS		0.0001	
	CMS+GRb1+GW vs. CMS+GRb1	6.878	< 0.0001	
Figure 2E-c	CMS vs. Ctrl		0.0695	
	GRb1 vs. Ctrl	0.380	0.0732	6
	CMS+GRb1 vs. CMS		0.0056	

	CMS+GRb1+GW vs. CMS+GRb1	0.6611
		0.445

Figure 2F-h	CMS vs. Ctrl		0.0142	
	GRb1 vs. Ctrl	1.530	0.3609	6
	CMS+GRb1 vs. CMS		0.0017	
	CMS+GRb1+GW vs. CMS+GRb1		0.0482	
		2.139		
Figure 2F-c	CMS vs. Ctrl		0.0151	
	GRb1 vs. Ctrl	1.862	0.4787	6
	CMS+GRb1 vs. CMS		0.9884	
	CMS+GRb1+GW vs. CMS+GRb1	0.933	0.3783	
Figure 2G-1	CMS vs. Ctrl		<0.0001	
	GRb1 vs. Ctrl	1.443	0.7468	5
	CMS+GRb1 vs. CMS		0.0057	
	CMS+GRb1+GW vs. CMS+GRb1		0.0013	
		4.834		5
Figure 2G-2	CMS vs. Ctrl		0.0329	
	GRb1 vs. Ctrl	3.340	0.8778	5
	CMS+GRb1 vs. CMS		0.0015	
	CMS+GRb1+GW vs. CMS+GRb1		0.0069	
		3.610		5
Figure 2H-1	CMS vs. Ctrl		0.0109	
	GRb1 vs. Ctrl	9.361	0.8942	5
	CMS+GRb1 vs. CMS		0.0004	
	CMS+GRb1+GW vs. CMS+GRb1		0.0028	
		4.258		5
Figure 2H-2	CMS vs. Ctrl		0.0159	
	GRb1 vs. Ctrl	6.216	0.6888	5
	CMS+GRb1 vs. CMS		0.0011	
	CMS+GRb1+GW vs. CMS+GRb1		0.0037	

		4.040		5
Figure 2I-1	CMS vs. Ctrl		0.0003	
	GRb1 vs. Ctrl	6.799	0.9950	5
	CMS+GRb1 vs. CMS		0.0048	
	CMS+GRb1+GW vs. CMS+GRb1		0.1812	
		1.464		5
Figure 2I-2	CMS vs. Ctrl		0.0005	
	GRb1 vs. Ctrl	30.290	0.2315	5
	CMS+GRb1 vs. CMS		< 0.0001	
	CMS+GRb1+GW vs. CMS+GRb1		0.0294	
		2.646		5
Figure 2J-1	CMS vs. Ctrl		0.0073	
	GRb1 vs. Ctrl	11.820	0.9568	5
	CMS+GRb1 vs. CMS		0.0002	
	CMS +GRb1+GW vs. CMS+GRb1		< 0.0001	
		7.331		5
Figure 2J-2	CMS vs. Ctrl		0.0282	
	GRb1 vs. Ctrl	16.090	0.3674	5
	CMS+GRb1 vs. CMS		0.0010	
	CMS+GRb1+GW vs. CMS+GRb1		0.0123	
		3.215		5

h, hippocampus; c, cortex

Table 3The F value and P value in multiple comparisons of figure 3

figure	group	F or T	P	N
Figure 3B	CMS vs. Ctrl		0.0008	
	GRb1 vs. Ctrl	27.880	0.2877	5
	CMS+GRb1 vs. CMS		< 0.0001	
	CMS+GRb1+GW vs. CMS+GRb1	7.291	< 0.0001	
Figure 3C	CMS vs. Ctrl		< 0.0001	
	GRb1 vs. Ctrl	47.020	0.7149	6
	CMS+GRb1 vs. CMS		< 0.0001	
	CMS+GRb1+GW vs. CMS+GRb1	8.922	< 0.0001	
Figure 3D	CMS vs. Ctrl		< 0.0001	
	GRb1 vs. Ctrl	30.200	0.9995	6
	CMS+GRb1 vs. CMS		< 0.0001	
	CMS+GRb1+GW vs. CMS+GRb1	6.145	0.0003	
Figure 3E	CMS vs. Ctrl		< 0.0001	
	GRb1 vs. Ctrl	4.820	0.9971	6
	CMS+GRb1 vs. CMS		0.0094	
	CMS+GRb1+GW vs. CMS+GRb1	3.659	0.0064	
Figure 3G	CMS vs. Ctrl		0.0399	
	GRb1 vs. Ctrl	10.990	0.4946	6
	CMS+GRb1 vs. CMS		0.0021	
	CMS+GRb1+GW vs. CMS+GRb1	2.858	0.0212	
Figure 3H	CMS vs. Ctrl		0.5954	
	GRb1 vs. Ctrl	1.460	0.8912	6
	CMS+GRb1 vs. CMS		0.0934	

	CMS+GRb1+GW vs. CMS+GRb1		0.1439	
		1.528		
Figure 3I	CMS vs. Ctrl		0.4818	
	GRb1 vs. Ctrl	3.167	0.9986	6
	CMS+GRb1 vs. CMS		0.0378	
	CMS+GRb1+GW vs. CMS+GRb1		0.0062	
		3.678		

Table 4 The F value and P value in multiple comparisons of figure 4

figure	group	F or T	P	N
Figure 4A	CMS vs. Ctrl		0.0174	
	GRb1 vs. Ctrl	2.407	0.6867	5
	CMS+GRb1 vs. CMS		< 0.0001	
	CMS+GRb1+GW vs. CMS+GRb1		0.0007	
		5.368		5
Figure 4B	CMS vs. Ctrl		0.9993	
	GRb1 vs. Ctrl	3.246	0.3731	5
	CMS+GRb1 vs. CMS		0.0422	
	CMS+GRb1+GW vs. CMS+GRb1		0.2723	
		1.179		5
Figure 4E-1	CMS vs. Ctrl		0.0119	
	GRb1 vs. Ctrl	9.619	0.9997	5
	CMS+GRb1 vs. CMS		0.0010	
	CMS+GRb1+GW vs. CMS+GRb1		0.0026	
		4.306		5
Figure 4E-2	CMS vs. Ctrl		0.0003	
	GRb1 vs. Ctrl	2.197	0.0913	5
	CMS+GRb1 vs. CMS		0.0147	
	CMS+GRb1+GW vs. CMS+GRb1		0.0009	
		4.670		5
Figure 4F-1	CMS vs. Ctrl		0.0134	
	GRb1 vs. Ctrl	2.242	0.9577	5
	CMS+GRb1 vs. CMS		0.0590	
	CMS+GRb1+GW vs. CMS+GRb1		0.3443	
		1.005		5
Figure 4F-2	CMS vs. Ctrl		0.1676	
	GRb1 vs. Ctrl	7.645	0.9676	5
	CMS+GRb1 vs. CMS		0.0538	

	CMS+GRb1+GW vs. CMS+GRb1		0.0067	
		3.692		5
Figure 4I	CMS vs. Ctrl		<0.0001	
	GRb1 vs. Ctrl	33.790	0.9944	5
	CMS+GRb1 vs. CMS		<0.0001	
	CMS+GRb1+GW vs. CMS+GRb1		0.0026	
		4.299		5
Figure 4J	CMS vs. Ctrl		0.1916	
	GRb1 vs. Ctrl	5.065	0.1499	5
	CMS+GRb1 vs. CMS		0.3793	
	CMS+GRb1+GW vs. CMS+GRb1		0.4853	
		0.732		5

Table 5 The F value and P value in multiple comparisons of figure 5

figure	group	F or T	P	N
Figure 5B	LPS vs. Ctrl		0.0175	
	GRb1 vs. Ctrl	0.101	0.0331	5
	LPS+GRb1 vs. LPS		0.0131	
	LPS+GRb1+GW vs. LPS+GRb1	2.352	0.0318	
Figure 5C	LPS vs. Ctrl		< 0.0001	
	GRb1 vs. Ctrl	16.850	0.9873	5
	LPS+GRb1 vs. LPS		< 0.0001	
	LPS+GRb1+GW vs. LPS+GRb1	2.953	0.0112	
Figure 5D	LPS vs. Ctrl		< 0.0001	
	GRb1 vs. Ctrl	25.380	0.1650	5
	LPS+GRb1 vs. LPS		< 0.0001	
	LPS+GRb1+GW vs. LPS+GRb1	1.615	0.1150	
Figure 5G	LPS vs. Ctrl		< 0.0001	
	GRb1 vs. Ctrl	20.280	0.2200	5
	LPS+GRb1 vs. LPS		< 0.0001	
	LPS+GRb1+GW vs. LPS+GRb1	1.514	0.1523	
Figure 5H	LPS vs. Ctrl		< 0.0001	
	GRb1 vs. Ctrl	26.160	0.7954	5
	LPS+GRb1 vs. LPS		< 0.0001	
	LPS+GRb1+GW vs. LPS+GRb1	5.004	0.0002	
Figure 5I	LPS vs. Ctrl		0.7890	
	GRb1 vs. Ctrl	1.794	0.0089	5
	LPS+GRb1 vs. LPS		0.2532	

	LPS+GRb1+GW vs. LPS+GRb1	0.396	0.6983	
Figure 5J	LPS vs. Ctrl	29.610	0.0001	5
	GRb1 vs. Ctrl		0.4226	
	LPS+GRb1 vs. LPS		< 0.0001	
	LPS+GRb1+GW vs. LPS+GRb1	5.007	0.0001	

Table 6 The F value and P value in multiple comparisons of figure S1

figure	group	F	P	N
Figure 6B-1	LPS vs. Ctrl	18.940	0.0454	6
	10 μg/ml LPS+GRb1 vs. LPS		0.4097	
	20 μg/ml LPS+GRb1 vs. LPS		< 0.0001	
	40 μg/ml LPS+GRb1 vs. LPS		> 0.9999	
Figure 6B-2	LPS vs. Ctrl	6.515	0.0100	6
	10 μg/ml LPS+GRb1 vs. LPS		0.0042	
	20 μg/ml LPS+GRb1 vs. LPS		0.0014	
	40 μg/ml LPS+GRb1 vs. LPS		0.0055	
Figure 6C-1	LPS vs. Ctrl	37.831	< 0.0001	6
	10 μg/ml LPS+GRb1 vs. LPS		< 0.0001	
	20 μg/ml LPS+GRb1 vs. LPS		< 0.0001	
	40 μg/ml LPS+GRb1 vs. LPS		< 0.0001	
Figure 6C-2	LPS vs. Ctrl	8.756	0.0133	6
	10 μg/ml LPS+GRb1 vs. LPS		0.0258	
	20 μg/ml LPS+GRb1 vs. LPS		0.0002	
	40 μg/ml LPS+GRb1 vs. LPS		0.0002	
Figure 6D	LPS vs. Ctrl	4.800	0.0357	12
	10 μg/ml LPS+GRb1 vs. LPS		0.9795	
	20 μg/ml LPS+GRb1 vs. LPS		0.0083	
	40 μg/ml LPS+GRb1 vs. LPS		0.9179	
Figure 6E	LPS vs. Ctrl	25.740	< 0.0001	12
	10 μg/ml LPS+GRb1 vs. LPS		0.9891	
	20 μg/ml LPS+GRb1 vs. LPS		< 0.0001	
	40 μg/ml LPS+GRb1 vs. LPS		< 0.0001	
Figure 6F	LPS vs. Ctrl	10.021	0.0284	6
	10 μg/ml LPS+GRb1 vs. LPS		0.0113	

	20 μg/ml LPS+GRb1 vs. LPS		< 0.0001	
	40 μg/ml LPS+GRb1 vs. LPS		0.0013	
Figure 6G	LPS vs. Ctrl		0.0404	
	10 μg/ml LPS+GRb1 vs. LPS	10.740	0.9650	10
	20 μg/ml LPS+GRb1 vs. LPS		< 0.0001	
	40 μg/ml LPS+GRb1 vs. LPS		0.0105	

Figures

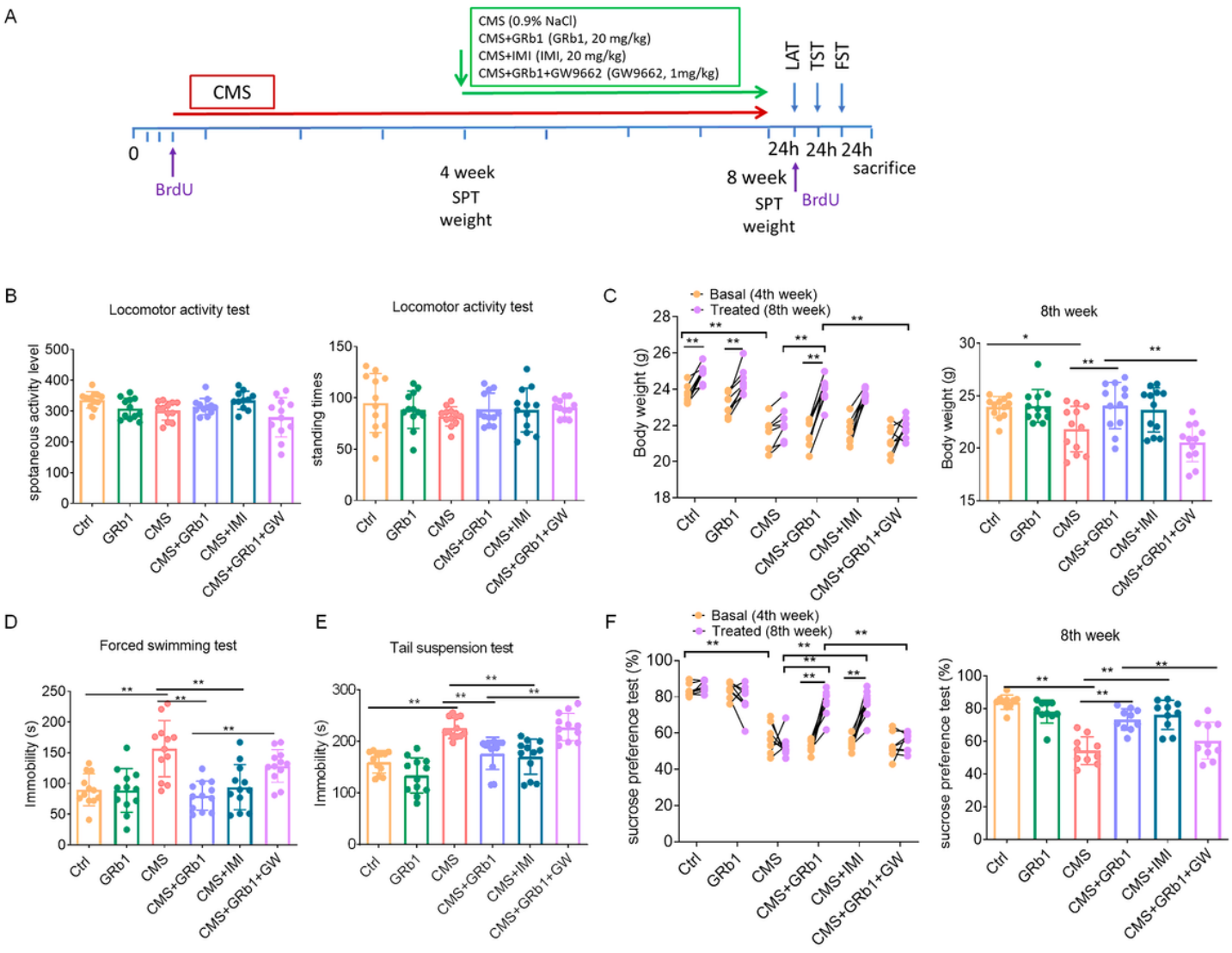

Figure 1

GRb1 alleviates depressive-like behaviors in male mice exposed to CMS. (a) Drug treatment protocol. (b) Locomotor activity at week 8. (c) Comparison of body weight between week 4 and 8, and comparison of weight at week 8 among the groups. (d–e) Duration of immobility in the forced swimming and tail

suspension tests at week 8. (f) Comparison of sucrose preference between week 4 and 8, and comparison of preference at week 8 among the groups (n = 12 mice/group). The statistical analysis results are shown in Table 1. *P < 0.05, ** p < 0.01.

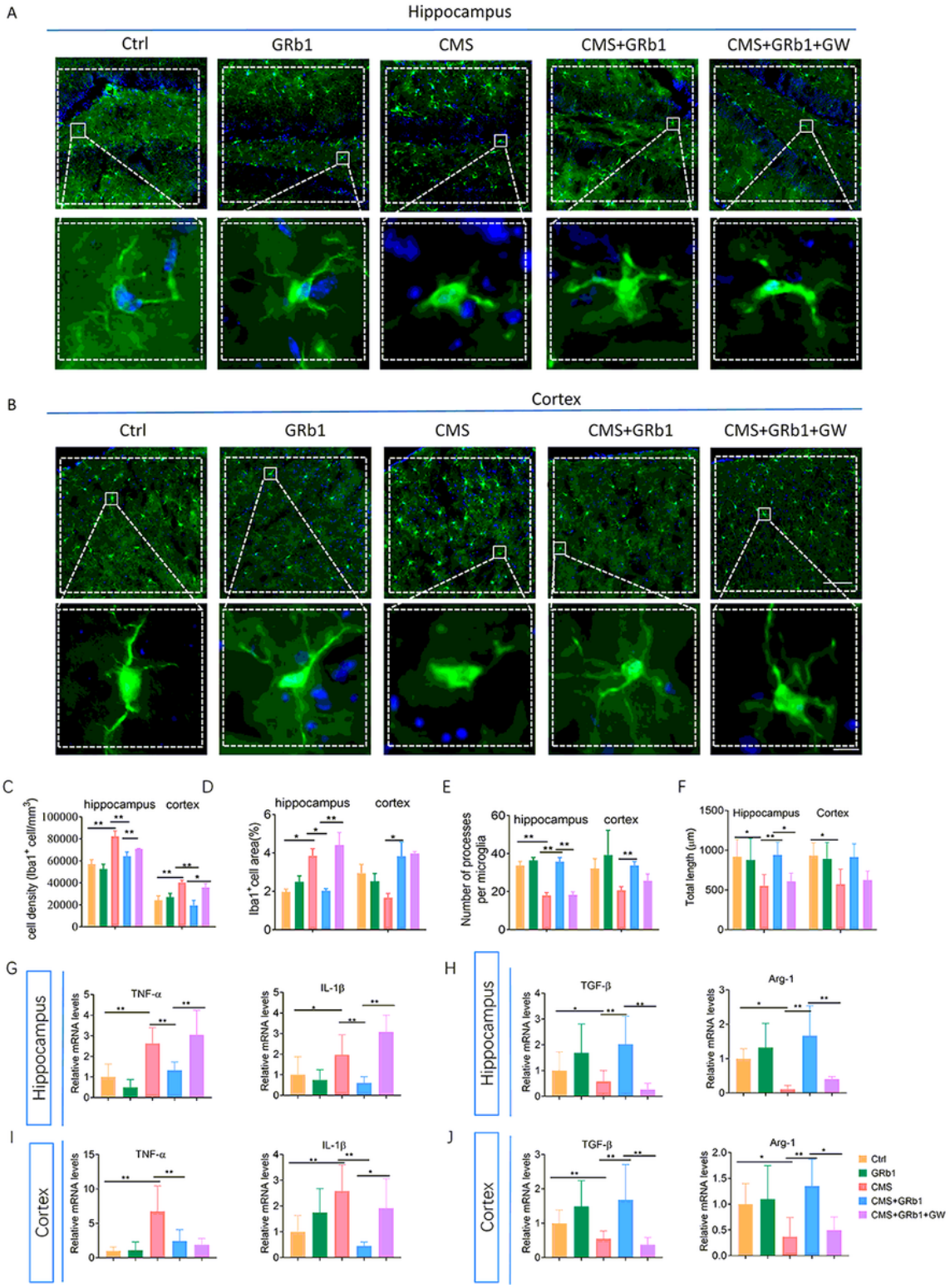

Figure 2

GRb1 reverses the effects of CMS on microglial phenotype and cytokine profile in mice. (a–b) Iba1+ cells in the hippocampus and cortex were quantified by immunofluorescence. Microglial morphology was

quantified by cell density (c), cell area (d), the number of processes per cell (e), and total length of processes per cell (f) (n = 6 mice/group). (g) Levels of pro-inflammatory microglial markers (TNF-α, IL-1β) in hippocampus. (h) Levels of anti-inflammatory microglial markers (TGF-β, Arg-1) in hippocampus (n = 5 mice/group). (i–j) Changes in levels of pro- and anti-inflammatory mediators in cortex (n = 5 mice/group). Scale bars, 50 μm (upper row in each panel), 10 μm (lower row in each panel). The statistical analysis results are shown in Table 2. *P < 0.05, ** p < 0.01.

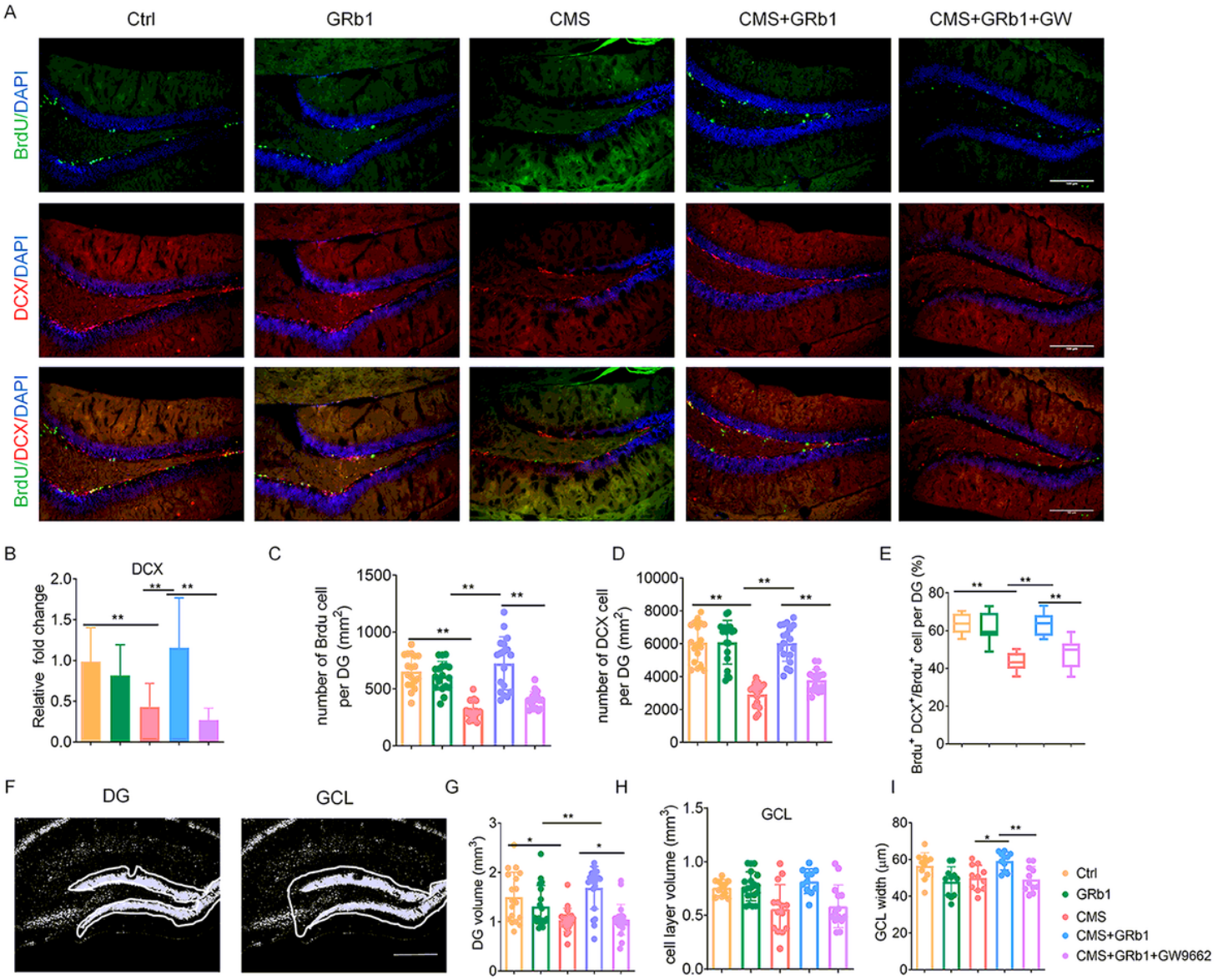

Figure 3

GRb1 rescues neurogenesis in the hippocampus of mice exposed to CMS. (a) Immunohistochemistry for DCX and BrdU in DG. (bB) Levels of DCX mRNA in DG (n = 5 mice/group). (c–d) Number of BrdU+ or DCX+ cells in DG. (e) Differentiation ratio of proliferative cells in DG. (f) DAPI-stained sections of DG and GCL, which were quantified by measure DG volume (g), GCL volume (h), and GCL thickness (i). Scale bars: 100 μm. Data are shown as mean ± SEM (n = 6 mice/group). The statistical analysis results are shown in Table 3. *P < 0.05, ** p < 0.01.

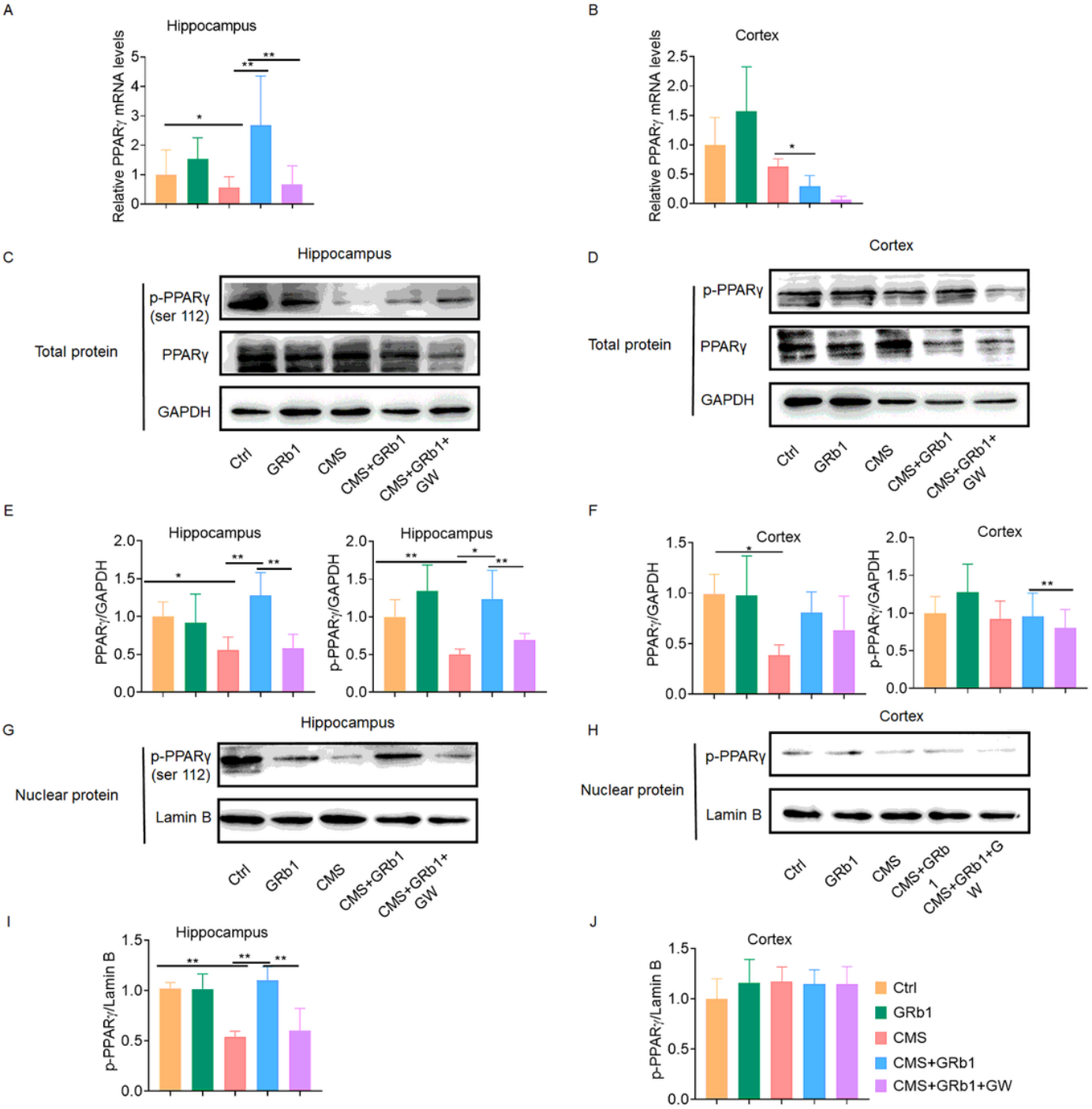

Figure 4

GRb1 rescues PPARγ expression in mice exposed to CMS. (a–b) Relative PPARγ mRNA levels in the hippocampus and cortex. (c–d) Representative western blot of p-PPARγ and PPARγ in hippocampus and cortex. (e–f) Quantification of PPARγ and p-PPARγ in hippocampus and cortex. (g–h) Representative western blot of p-PPARγ in nuclei of hippocampus and cortex. (i–j) Quantification of p-PPARγ in nuclei of hippocampus and cortex (n = 5 mice/group). The statistical analysis results are shown in Table 4. *P < 0.05, ** p < 0.01.

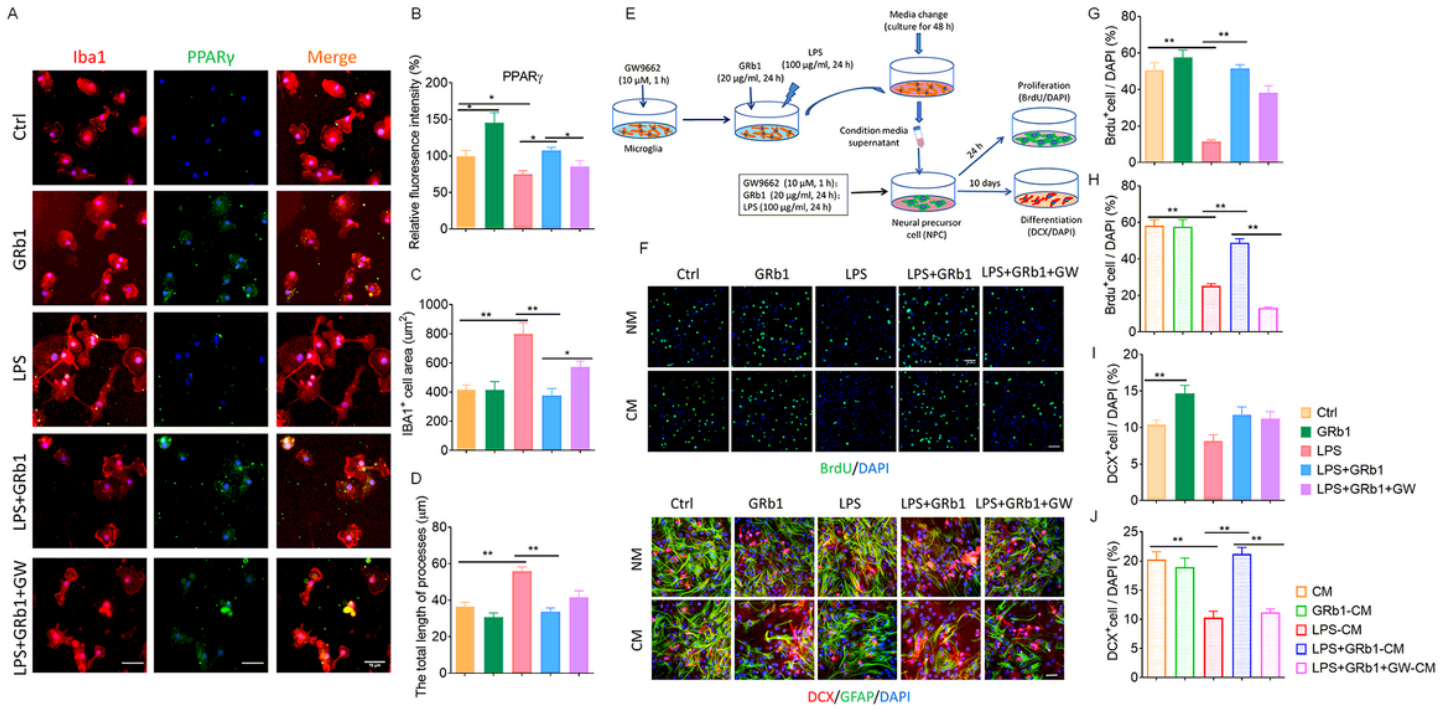

Figure 5

PPARγ-dependent pathways mediate effects of GRb1 in vitro. (a) Representative micrographs after immunostaining against Iba1 display microglial activation phenotype. Fluorescence intensity reflects PPARγ expression. Scale bars: 20 μm. (b) Quantitation of PPARγ fluorescence intensity, (c) unbiased stereological quantification of microglial cell area, and (d) total length of processes. (e) Experimental protocol to test the effects of conditioned medium from microglial cultures on neural precursor cell (NPC) cultures. (f) NPCs cultures were maintained in native medium (NM) and directly stimulated by GRb1, LPS, and GW9662; or they were maintained in conditioned medium (CM) of activated microglia. After 1 day or 10 days, the proliferation and differentiation of NPCs were tested, respectively, by immunolabeling BrdU (upper two rows) or DCX and GFAP (lower two rows). Scale bars: 15 μm. (g–h) The ratio of BrdU+ to DAPI+ cells in NPCs cultures maintained in native medium or exposed to conditioned medium from microglial cultures. (i–j) The ratio of DCX+ to DAPI+ cells in NPCs cultures maintained in native medium or exposed to conditioned medium. The statistical analysis results are shown in Table 5. *P < 0.05, ** p < 0.01.

Supplementary Files

This is a list of supplementary files associated with this preprint. Click to download.

- Onlinefig.S1.png